Supplementary Figures

Supplementary Figure 1: Resting Calcium in Cultured Neurons

A) Multiphoton image of a cultured neuron expressing YC3.6. B) Resting calcium in a proximal dendrite of a neuron was calculated to be 41 +/- 7 nM (n = 5 dishes, n = 48 neurons).

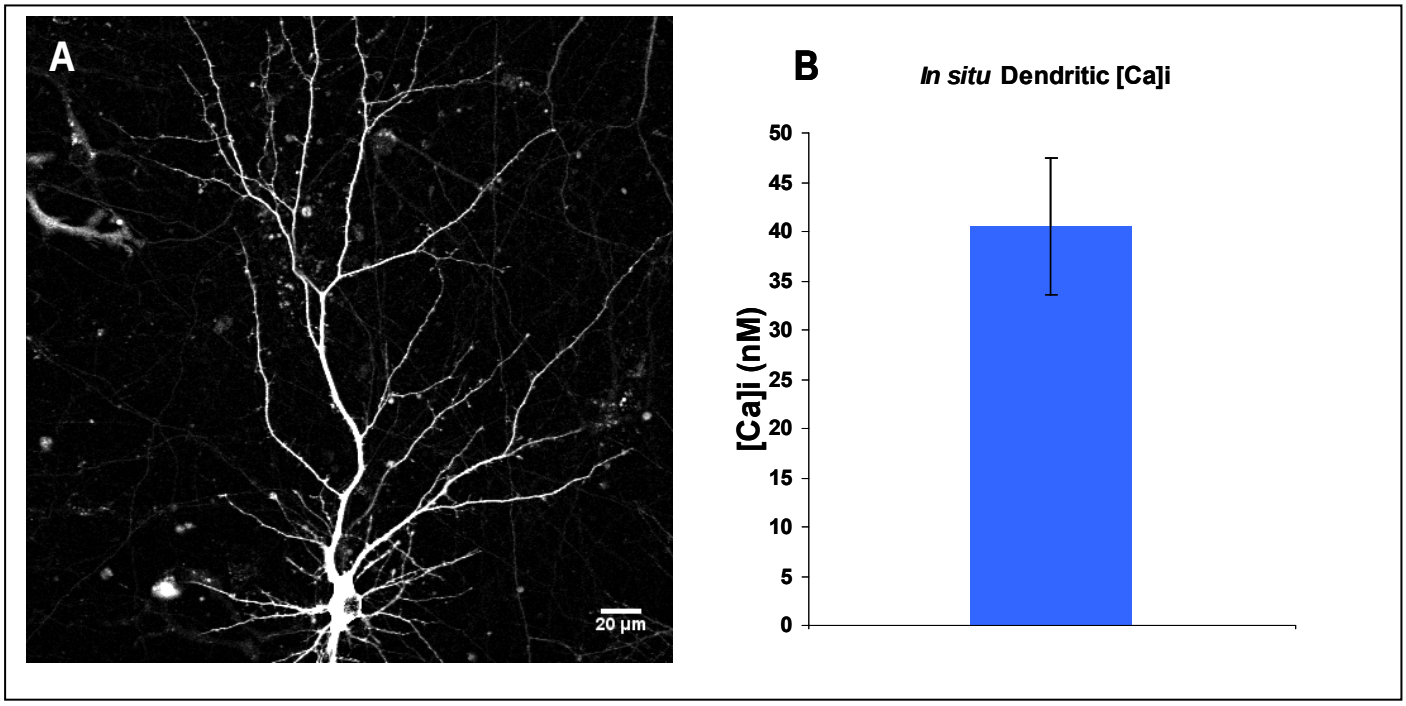

Supplementary Figure 2: YC3.6 Accurately Reports Somatic Spontaneous Activity in vivo

A) A multiphoton image of layer 5 pyramidal neurons *in vivo* (~400 uM below the surface of the brain). We observed calcium transients in all 5 mice in which we were able to make stable recordings. Data was analyzed for two of these mice which we sampled at ~5.3 Hz—for the others we used a sampling rate of 2.5Hz which was insufficient to fully characterize the fast kinetics of the probe. B) Spontaneous calcium

transients are visible with YC3.6—data is presented as ΔR/R, i.e. the change in ratio compared to baseline. This trace covers 75 seconds sampled at 188 ms/frame (~5.3 Hz). Notice the relatively sharp rise and decay of the independent transients (timecourses are low-pass filtered and smoothed for display purposes only, not for data analysis). C) The peak of the somatic calcium transients, characterized as the maximum value during the spontaneous burst, was robust and consistent (ΔR/R = 68.7 +/- 3.8 %, n = 68 transients in 2 mice). The "average" calcium rise, defined as the total change in ratio during the course of the spontaneous burst, is also described (ΔR/R = 39.2 +/- 3.0%, n = 68 transients in 2 mice). D) The temporal kinetics of the probe were surprisingly fast. The average duration of the spontaneous transient was characterized to be 0.862 +/- 0.055 seconds (n = 68 transients in 2 mice) and the decay (τ_{decay}) from the peak was 0.434 +/- 0.045 seconds. These data provide evidence that physiological calcium signals can be

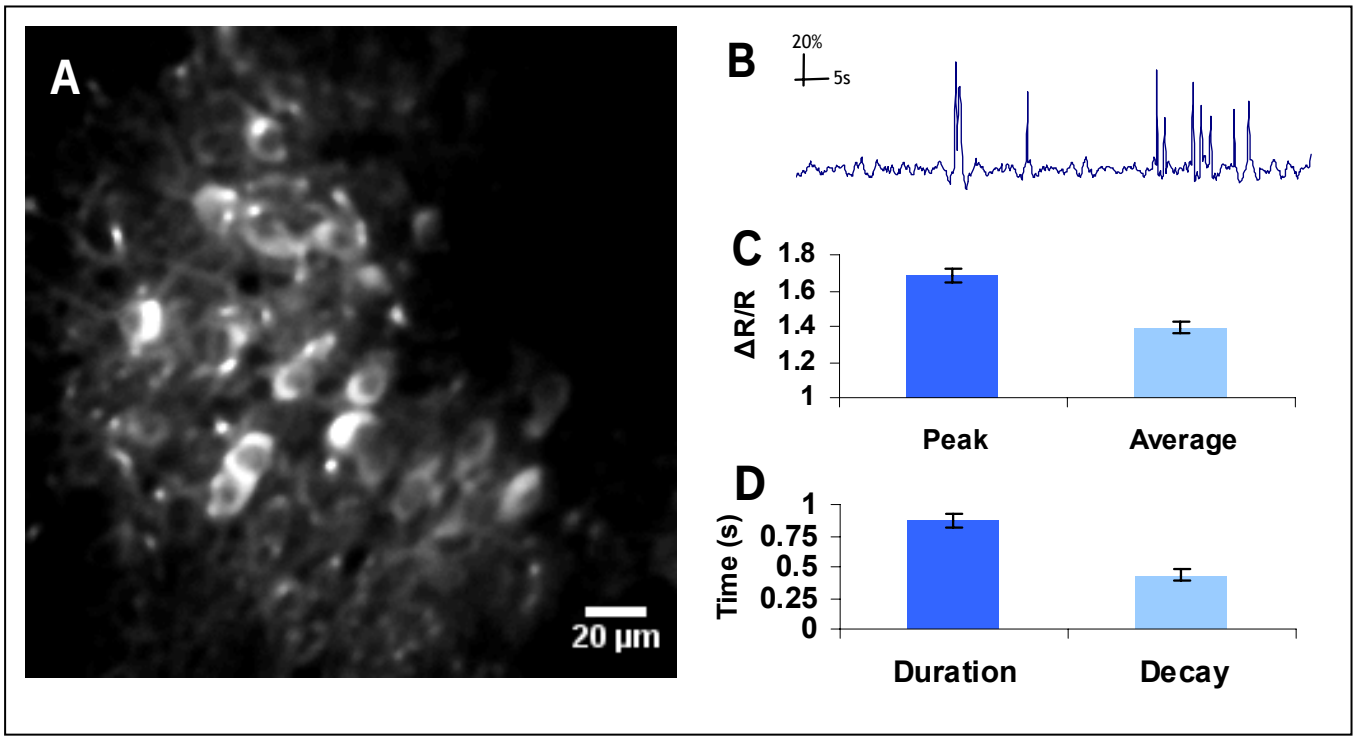

recorded and measured quantitatively with YC3.6.

Supplementary Figure 3: APP/PS1 Transgenic Mice do not Exhibit Calcium Overload Before Plaque Deposition

A) Representative multiphoton image of dendrites and axons in layer 1 of the neocortex in APP/PS1 transgenic mice before plaque deposition (3-3.5 mo-old). B) Distribution of neuritic [Ca]i in plaque-free 3-3.5 mo-old APP/PS1 transgenic mice (blue bars) compared to APP/PS1 transgenic mice with plaques (> 6.0 mo-old, red line). The distributions are significantly different (**, p < 0.001, Student's T-test) and the young mice have only 2.3% of all neurites with [Ca]i greater than 147 nM. C) Calcium overload

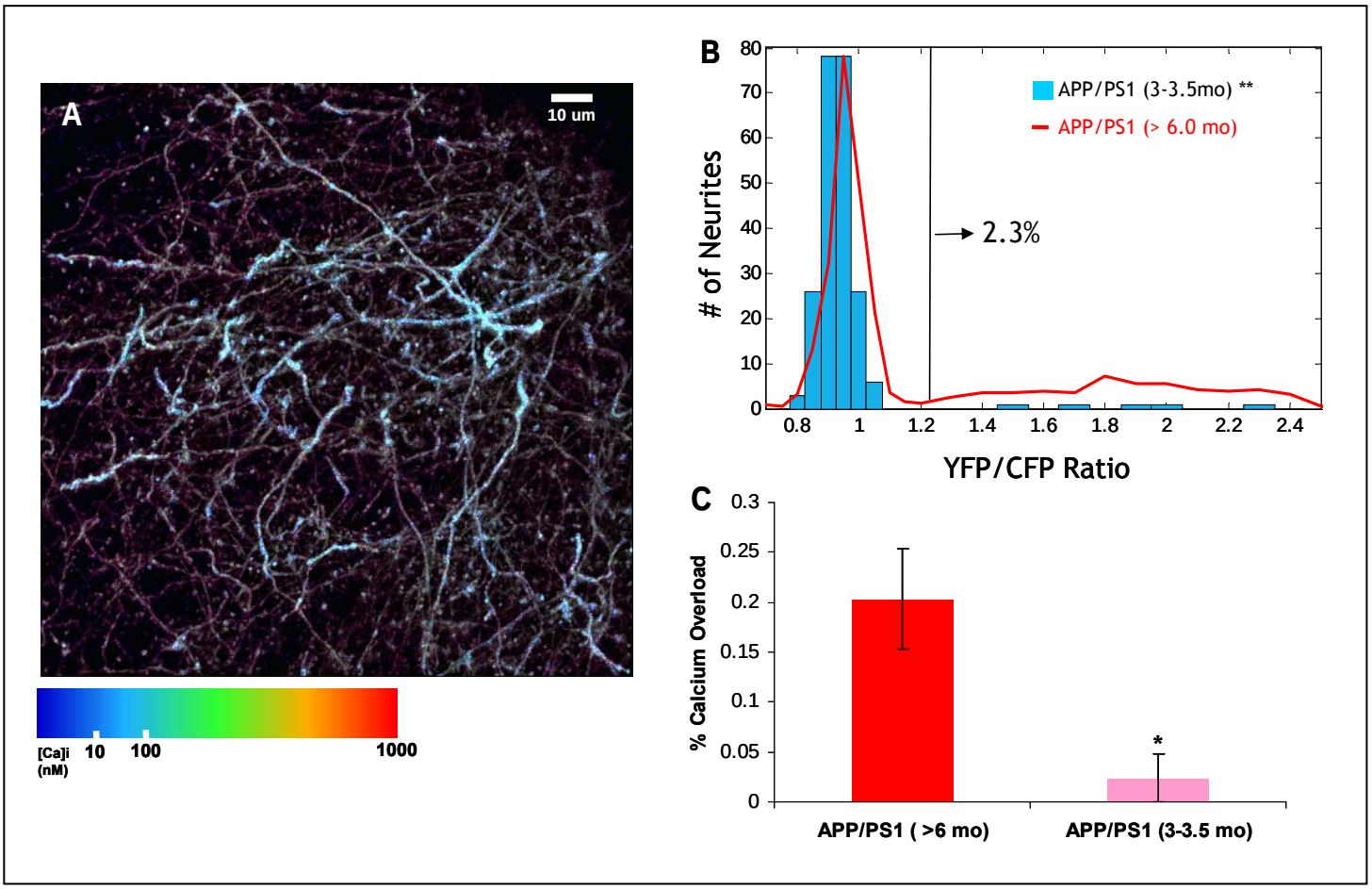

is significantly less (*, $p < 0.05$) in transgenic mice before plaque deposition.

Supplementary Figure 4: Tg-2576 transgenic mice (APPswe) Exhibit Abundant Calcium Overload

A) Multiphoton image of calcium-overloaded neurites in a tg-2576 transgenic mouse. This mouse carries the APPswe mutation and develops plaques at an older age when compared to the APP/PS1 mouse line (~14-15 months). As can be seen, like in the APPswe/PS1DE9 mice, there are a large number of calcium overloaded processes. B) Multiphoton image of an age-matched tg-2576 non-transgenic mouse—there are minimal processes exhibiting calcium overload. C) Histogram of dendritic and axonal YFP/CFP ratio showing that 22.1% of all neurites in the transgenic mice exhibit calcium overload—a number similar to that seen in the APP/PS1 mice. D) In the non-transgenic mice, only 4.5% of neurites cross the calcium-overload threshold.

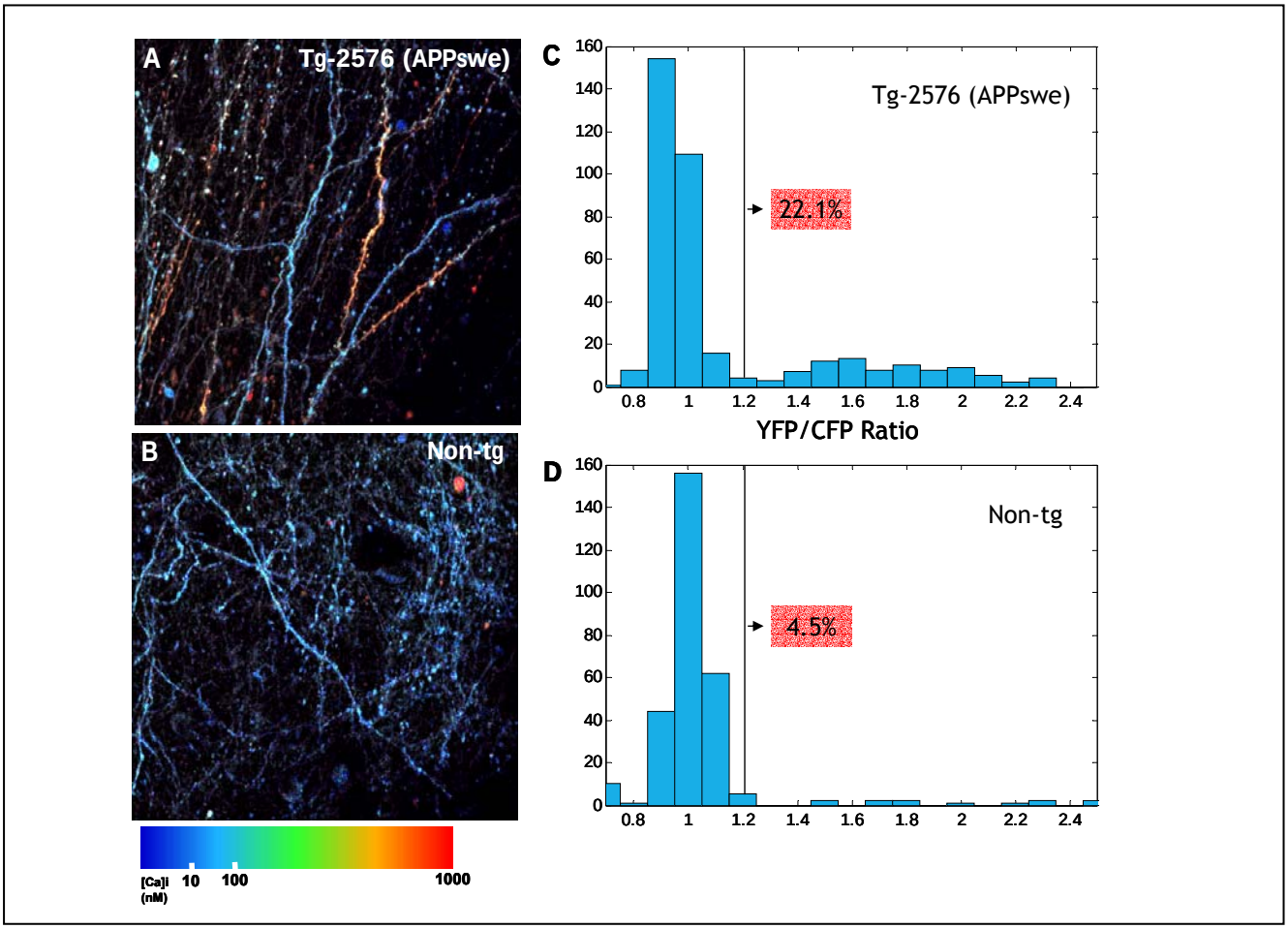

Supplementary Figure 5: PS1-ΔE9 Transgenic Mice do not Exhibit Calcium Overload

A) Representative multiphoton image of dendrites in layer 1 of the neocortex of PS1-ΔE9 transgenic mice. The image is pseudocolored for [Ca]i. B) A histogram of YFP/CFP ratios for all those neurites that could be manually identified—note that there are only 2.6% of all neurites which exhibit calcium elevations which is not significantly different from control.

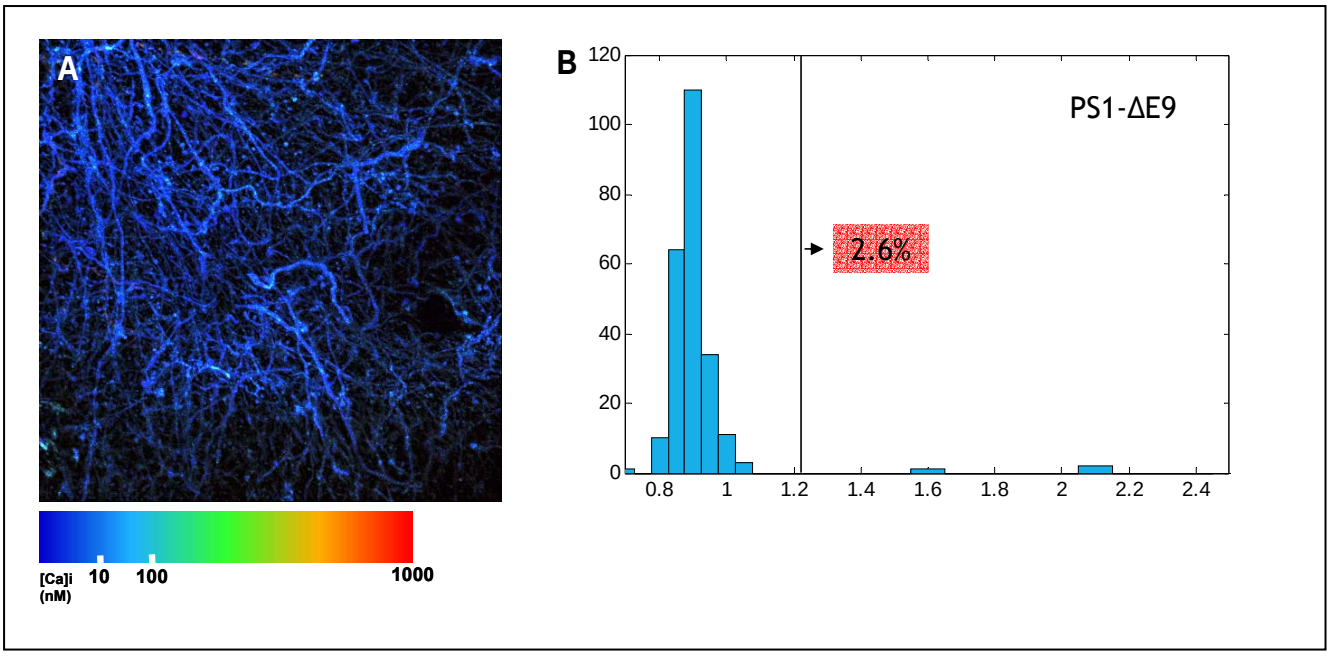

Supplementary Figure 6: Model of Neuronal Dysfunction and Degeneration in AD

A large number of dendrites and axons in transgenic mice with Aβ plaques experience [Ca]i-overload. A simple conceptual model, which is supported by our data, might explain how this leads to loss of network function in learning and memory. First, fibrillar and oligomeric Aβ trigger [Ca]i overload—yielding profound effects on intracellular and synaptic signaling. The resulting moderate calcium overload initiates a second pathological stage that activates the phosphatase, calcineurin. Increase CaN

activity then triggers the final stage of neurite structural degeneration and even more severe calcium overload. In one path, moderate but sustained [Ca]i-elevations might mimic LTD and lead to loss of synaptic contacts and spine density (as seen near senile plaques *in vivo* and upon application of Aβ *in situ*). An increase in LTD might underlie changes in network function that have implications for learning/memory. A reduction in the local Aβ concentration might ameliorate this problem. Simultaneously, a subset of [Ca]i-elevated neurites, both aspiny axons and spiny dendrites, continue to degenerate into neuritic beads. These neurites are unable to propagate signals through the network augmenting behavioral changes to learning and memory. This stage of degeneration can be partially prevented by CaN inhibition—which has been shown to restore associative learning and memory in Tg-2576 mouse models.